Interdisciplinary Sciences: Computational Life Sciences (2022) 14:596–606
https://doi.org/10.1007/s12539-022-00508-0

ORIGINAL RESEARCH ARTICLE

Development of Electrochemical Biosensor for miR204-Based Cancer Diagnosis

Shilpa Gundagatti[1] · **Sudha Srivastava**[1]

Received: 2 December 2021 / Revised: 11 February 2022 / Accepted: 17 February 2022 / Published online: 26 April 2022

Abstract

With increase in cancer burden worldwide and poor survival rates due to delayed diagnosis, it is pertinent to develop a device for early diagnosis. We report an electrochemical biosensor for quantification of miRNA-204 (miR-204) biomarker that is dysregulated in most of the cancers. The proposed methodology uses the gold nanoparticles-modified carbon screen-printed electrode for immobilization of single-stranded DNA probe against miR-204. Colloidal gold nanoparticles were synthesized using L-glutamic acid as reducing agent. Nanoparticles were characterized by UV–visible spectroscopy and transmission electron microscopy. Spherical gold nanoparticles were of 7–28 nm in size. Biosensor fabricated using these nanoparticles was characterized by cyclic voltammetry after spiking 0.1 fg/mL–0.1 µg/mL of miR-204 in fetal bovine serum. Response characteristics of the miR-204 biosensor displayed high sensitivity of 8.86 µA/µg/µL/cm^2 with wide detection range of 15.5 aM to 15.5 nM. The low detection limit makes it suitable for early diagnosis and screening of cancer.

Graphical abstract

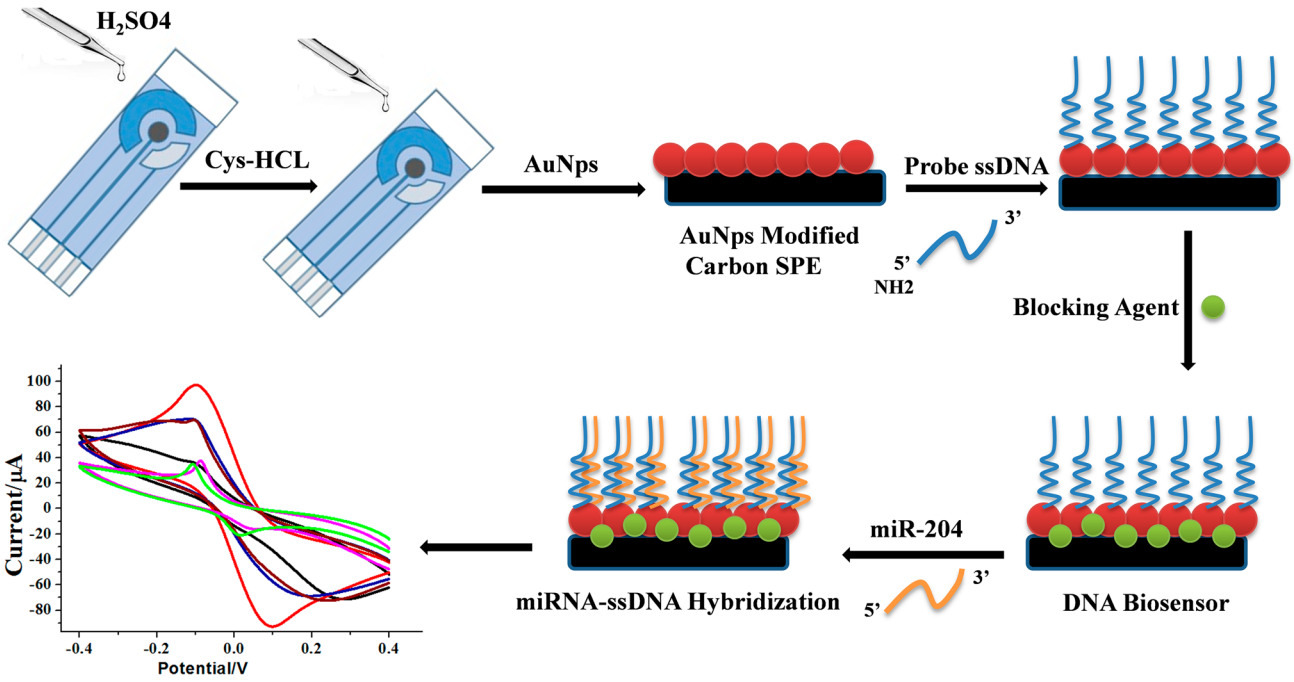

Keywords Biosensors · Cancer detection · miR-204 · Electrochemical detection · Early cancer diagnosis

✉ Sudha Srivastava
sudha.srivastava@jiit.ac.in

Extended author information available on the last page of the article

1 Introduction

In global analysis, cancer is reported to be the second major cause of death and ranks fourth in India [1]. As per GLOBOCAN 2020 statistics, cancer burden is expected to rise from 19.3 million in 2020 to approximately 28.4 million cases in 2040 [2]. Challenges are far greater in developing countries that have limited access to effective diagnostic services such as pathology, laboratory and imaging—all key to timely detection and treatment. Survival chances significantly decrease when cancer is detected at later stages. Classical tumor marker genes, proteins and epigenetic markers have low positivity and poor sensitivity in early stages of cancer. Hence, early diagnosis of cancer requires new paradigms in diagnostic technique as well as biomarker identification [3].

MicroRNAs (miRs) have emerged as a promising biomarker for early detection of tumors as well as other nonmalignant diseases [4]. These miRs are a short stretch of 19–25 nucleotide present in solid tissues as well as cell-free miRNA in different body fluids [5]. The abundant availability and high stability of miRNAs in tissue, blood, urine and other body fluids make it easy to detect with high sensitivity [6]. The miRNA can be upregulated or downregulated in a given pathological condition depending on the body fluid or solid tumor being studied. Presently, these miRNAs are detected by quantitative real-time RT-PCR, northern blotting, bead-based microarray, and deep-sequencing techniques which require trained manpower and laboratory facilities with high end costly instruments [7]. Electrochemical (bio)sensors seem to be a promising cost-effective alternative as point-of-care devices that can be easily operated by any individual [8].

The miR-204 has been reported in various cancers such as colon cancer, gastric cancer, breast cancer, glioma cancer, non-small cell lung cancer, endometrial cancer, papillary thyroid carcinoma, retinoblastoma intrahepatic cholangiocarcinoma, neuroblastoma, nephroblastoma, cervical cancer, bladder cancer, and colorectal cancer, as shown in Table 1. While other novel miRNA biomarkers that are reported are either specific or limited to few cancers only, miR-204 can be a potential candidate for screening of cancers. The dual role of miR-204 as tumor suppressor and oncomiR is reported in studies of upregulation/downregulation of specific genes by miR-204. In most of the studies, miR-204 is reported to be downregulated and its expression levels are inversely correlated with tumor progression. However, there are conflicting reports of over/underexpression of miR-204 in some of the solid tumors such as pancreatic [9], ovarian [10], endometrial [11], breast [12], prostate [13], and colorectal cancer [14]. Segregating studies based on samples studied and analysis of the results show downregulation of miR-204 in serum samples in different carcinomas [15–19], while it is upregulated in other diseases [20–23]. This agrees with cell lines-based studies that report downregulation of miR-204 in different cancer cell lines [29, 36–40], except one report on breast cancer cell line [41]. However, urine sample analysis shows elevated levels of miR-204 in cancerous condition [24, 25] and downregulated in other diseases [26]. However, tissue sample analysis shows conflicting reports, and based on miR-204 levels it is difficult to differentiate cancerous and other conditions [9, 12, 14, 27–35]. Hence, quantification of miR-204 levels in blood, serum, plasma or urine samples and evaluation of the deviation from standard/control samples can be used for screening of cancer.

The present study reports the development of an electrochemical biosensor for quantification of miR-204. Gold nanoparticles-modified carbon screen-printed electrodes were employed for immobilization of probe DNA against miR-204. The fabricated biosensor could detect miR-204 from 15.5 aM to 15.5 nM. The achieved low detection limit and role of miR-204 in almost all cancers make it a promising tool for screening of cancer.

2 Experimental

2.1 1Materials

Tetrachloroauric(III) acid and bovine serum albumin (BSA) from Himedia, trisodium citrate (TSC), potassium ferrocyanide, sodium dihydrogen phosphate, anhydrous sodium carbonate, disodium hydrogen phosphate, potassium chloride, sodium chloride, sodium bicarbonate, Tris–hydrochloride, ethylenediaminetetraacetic acid, polyethylene glycol 4000, and polyethylene glycol 6000 were purchased from CDH chemicals Ltd., cysteamine hydrochloride from Sigma-Aldrich and gelatin from Merck, USA. The ssDNA probe and miRNA were synthesized by Sigma-Aldrich: single-stranded probe DNA 5'-NH2-AGGCATAGGATGACAAAG GGAA3'and the miRNA-204 with the sequence of 5'UUC CCUUUGUCAUCCUAUGCCU3'.

2.2 Apparatus

The electrochemical measurements were performed using CHI-604E electrochemical workstation from CH Instruments, USA. It was employed for recording the cyclic voltammetric curves after addition of 100 µL of potassium ferri/ferrocyanide solution covering the entire three electrodes. Carbon screen-printed electrodes were from Gwent, comprising a three-electrode system consisting of a working electrode (C2070424P2 carbon graphite ink containing Prussian blue mediator, 3 mm in diameter) as well as a counter electrode made up of carbon and a reference electrode of Ag/AgCl. All electrochemical measurements were carried out in 100µL of 5 mM of potassium ferri/ferrocyanide 0.01 M PBS, pH 7.4.

Table 1 Representation of dual regulatory role of miR-204 in various cancers/diseases

Reference	Type of cancer/disease	Expression patterns of miR-204	Reported samples
Blood/serum/plasma samples			
Chen et al. [15]	Gastric cancer (GC)	**Downregulated**	Serum samples of GC patient
Wu et al. [16]	Endometrial cancer	**Downregulated**	serum
Zheng et al. [17]	Lung cancer	**Downregulated**	Serum sample of patient lung cancer
Nie et al. [18]	Acute myeloid leukemia (AML)	**Downregulated**	AML serum samples and Kasumi-1 and HL-60 cells
Guo et al. [19]	Non-small cell lung cancer (NSCLC)	**Downregulated**	Plasma patient of NSCLC
Gaddam et al. [20]	Non-dipping hypertension in diabetic patients (heart and kidney failure)	Upregulated	Blood
Cheng et al. [21]	Chronic kidney diseases	Upregulated	Blood
Chiu et al. [22]	Parkinson's diseases (PD)	Upregulated	Serum samples of PD patient
Xu et al. [23]	Type 1 diabetes	Upregulated	Serum sample
Urine samples			
Kurahashi et al. [24]	Renal cell carcinoma	**Upregulated**	Urinary exosomes of renal PRCCTFE3 Tg mice
Debernardi et al. [25]	Stage 1 pancreatic ductal adenocarcinoma	**Upregulated**	Urine sample of PDAC patient
Tapia-Castillo and Guanzon et al. [26]	High blood pressure	Downregulated	Urinary exosomes
Tissue samples			
Hofbauer et al. [27]	Kidney patients with hypertension, hypertensive nephrosclerosis, or diabetic nephropathy	Downregulated	Human kidney tissue
Scian et al. [28]	Chronic allograft dysfunction (CAD)	Downregulated	Kidney tissue samples
Turner et al. [29]	Prostate cancer	Upregulated	Tumor of prostate cancer patient
Li et al. [12]	Breast cancer	Downregulated	Breast cancer tissue
Lee et al. [30]	Breast cancer	Downregulated	Breast cancer tissue
Hong et al. [31]	Breast cancer	Downregulated	Breast cancer tissue
Hoffmann et al. [32]	Secondary cataract (SC)	Upregulated	Lens tissue
Sümbül et al. [14]	Colorectal cancer	Upregulated	Colorectal cancer tissue
Yin et al. [33]	Colorectal cancer	Downregulated	Colorectal cancer tissue
Khalid et al. [9]	Pancreatic ductal adenocarcinoma (PDAC)	Downregulated	PDAC tissue and cell lines SW1990 and PANC-1
Conte et al. [34]	Inherited retinal dystrophy associated with ocular coloboma	Downregulated	Eye tissue samples
Qiu et al. [35]	Intrahepatic cholangiocarcinoma (ICC)	Downregulated	Human ICC tissue and cell lines ICC-9810
Cell lines			
Shen et al. [36]	Breast cancer	Downregulated	Breast cancer MCF-7 cells
Guo et al. [37]	Bladder cancer (BC)	Downregulated	Urine sample of BC patients
Ding et al. [29]	Prostate cancer	Downregulated	PAC and NPEC cells
Ying et al. [38]	Glioma	Downregulated	SNB19 and LN382T glioma cell lines
Ryan et al. [39]	Neuroblastoma	Downregulated	Neuroblastoma cell lines
Zhang et al. [40]	Gastric Cancer(GC)	Downregulated	AGS and BGC gastric cancer cell lines
Findlay et al. [41]	Breast cancer	**Upregulated**	Breast cancer cell line MCF7 and human breast tumor

2.3 Gold Nanoparticle Synthesis Using L-Glutamic Acid

In the proposed methodology, the gold nanostructures were synthesized using modified Turkevich method as described by Shikha et al. [42]. In the experiment, 100 mL of 0.5 mM tetrachloroauric(III) acid prepared in deionized water (18.2 MΩ) in a conical flask was brought to boiling condition on a magnetic stirrer with heating. To the boiling chloroauric acid precursor solution, 3 mL of 100 mM L-glutamic acid was injected at a flow rate of 200 µL/min, while heating and vigorously stirring the solution. To minimize the evaporation

and contamination during synthesis, the flask was covered with a Petri dish which helps in achieving the objective.

2.4 Biosensor Fabrication

The schematic representation of the step-by-step biosensor fabrication for quantification of miR-204 is shown in Fig. 1. The working electrode of 2 mm diameter and counter electrode having area 5 mm (ratio of area working/counter electrode = 3) were of carbon, while reference electrode was made up of silver. The screen-printed carbon electrode was cleaned by treating the working electrode surface by 0.1 M sulfuric acid to remove pre-adsorbed impurities. The sulfuric acid-treated electrode was then washed with deionized water and completely air dried. This was followed by treatment of the working electrode surface with 7 µL cysteamine hydrochloride with the desired concentration (2 mg/mL) for 1 h under dark condition. This leads to the thiol-ene reaction(C = C–SH) thereby yielding thio-functionalized electrode surface. Excess of cysteamine hydrochloride was washed by rinsing the electrode with deionized water. Addition of 7µL of synthesized gold nanoparticles (AuNPs) onto the working electrode and incubation for 1 h at room temperature result in nanoparticles-catalyzed amide bond formation between the COO^- groups on the surface of AuNPs and NH_3^+ groups of cysteamine hydrochloride on the working electrode surface. Unbound gold nanoparticles are removed by washing with deionized water. The AuNPs-modified electrode surface is treated with 7µL of 0.5 µg/mL of ssDNA probe and incubated for 1 h at room temperature. The free citrate groups on the surface of AuNPs form amide linkage with amino-modified free 5' end of the ssDNA probe. Unbound or physically adsorbed probe was removed by washing with deionized water, followed by air drying under ambient conditions. Finally, the fabricated biosensor was treated with 1% gelatin, as a blocking agent to avoid non-specific interactions on the electrode surface. After 1 h of incubation with blocking agent at 37 °C, the electrodes were washed with deionized water and air dried. The total time taken for complete fabrication of DNA-based biosensor is about 4 h.

2.5 Electrochemical Measurements

Cyclic voltammetry (CV) was employed to determine the electrochemical properties of the fabricated DNA-based biosensor. Electrochemical measurement was done by adding 100 µL of 5 mM ferri/ferrocyanide solution onto the fabricated biosensor surface covering all three working, reference and counter electrodes. A sweeping potential of −0.9 to 0.9 V at a scan rate of 100 mV/s was applied and a cyclic voltammogram was recorded. Response characteristics of the biosensor were evaluated by preparing different concentrations of miR-204 (0.1 fg/mL–0.1 µg/mL) spiked in fetal bovine serum (FBS) and recording the cyclic voltammogram in a suitable potential window.

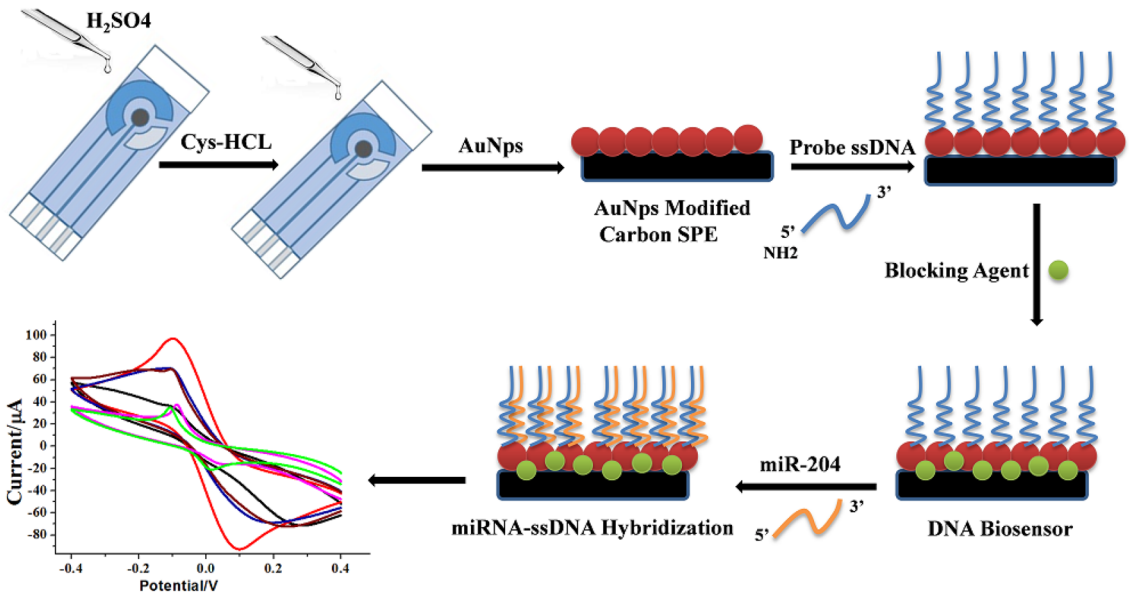

Fig. 1 Schematic representation of stepwise DNA-based biosensor fabrication

3 Results and Discussion

3.1 Gold Nanoparticles

Colloidal gold nanoparticles synthesized using L-glutamic acid were characterized by transmission electron microscopy and UV–visible absorption spectroscopy. Transmission electron microscopic image shows spherical nanoparticles of 7–28 nm in size as shown in Figure 2a. The absorption spectra of the colloidal suspension show an absorption peak with maxima at 528 nm. The choice of the gold nanoparticles for biosensor development was dictated by performance parameters such as sensitivity, detection range, and stability or reproducibility of the biosensor. Gold nanoparticles improve the sensitivity of the biosensor owing to high conductivity and at the same time not having oxidation issues like silver and copper nanoparticles. In addition to this, the usage of nanoparticles in general for biosensor fabrication leads to increase in the effective surface area of the electrode. This helps in increasing the loading capacity of the probe DNA (biorecognition molecule) without increasing the size of the biosensor. Increased loading capacity is in turn responsible for a wider detection range of the biosensor.

3.2 Biosensor Characterization

The biosensor fabrication/surface functionalization at each step was confirmed by cyclic voltammetry (CV) response analysis. Figure 3 shows voltammogram of carbon screen-printed electrode (CSPE) recorded in 0.5 mM ferri/ferro cyanide solution in a potential window of −0.4 to 0.4 V. As observed from Fig. 3, bare CSPE (black solid line) shows redox peaks at cathodic potential of −0.115 V (E_{PC}) and anodic potential of 0.2623 V (E_{PA}) and the corresponding peak currents were 37.02 µA (I_{PC}) and −60.59 µA (I_{PA}). After surface functionalization of carbon screen-printed electrode with cysteamine hydrochloride, the cathodic and anodic peak current increased to 96.2 µA (I_{PC}) and 92.7 µA (I_{PA}), due to ionic character of cysteamine hydrochloride (red-colored dash). Immobilization of gold nanoparticles onto cysteamine-modified CSPE results in decrease in the peak current to 69.54 µA (I_{PC}) and −68.14 µA (I_{PA}) (blue-colored dot) due to the semiconducting nature of gold nanoparticles. Finally, after immobilization of the single-stranded probe DNA, negligible change in peak current is observed (I_{PC}: −69.4 µA and I_{PA}: −58.83 µA) since ssDNA is a charged biomolecule (brown-colored dash dot). Hence, despite having insulating character of biomolecules, the expected reduction in current is not observed since DNA is a charged molecule. Blocking the electrode surface with gelatin increases the insulating character, hence a sharp decline

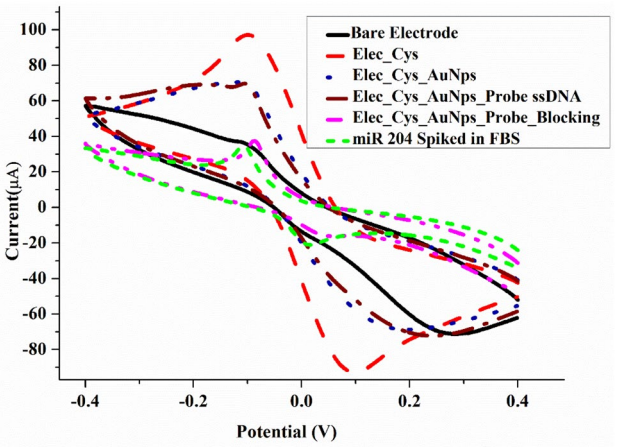

Fig. 3 Cyclic voltammetry of carbon screen-printed electrodes after modification with CysHCl, AuNPs, probe, blocking buffer and miR-204

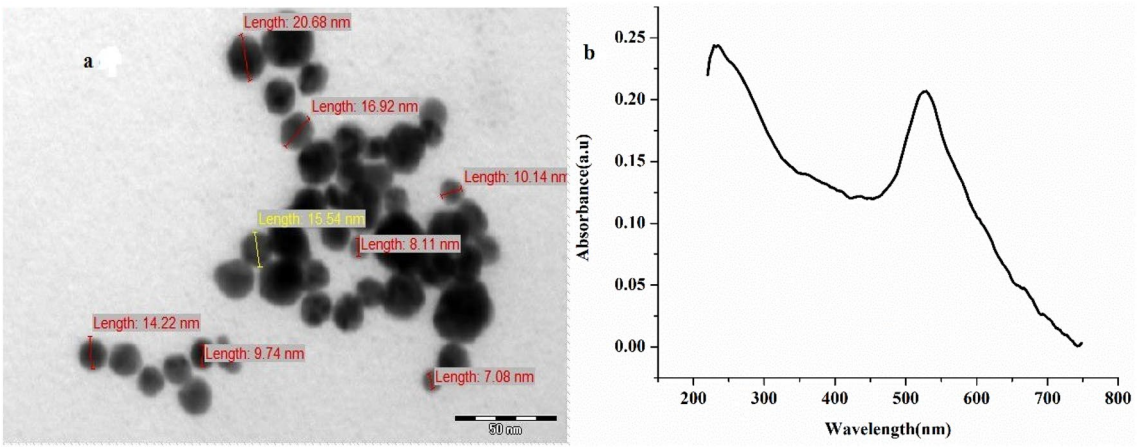

Fig. 2 **a** TEM micrograph of gold nanoparticles synthesized using L-glutamic acid as reducing agent, **b** UV–visible absorption spectra of synthesized gold nanoparticles

in peak current is observed with I_{PC} as 30.4 µA and I_{PA} as 12.78 µA (magenta-colored dash dot dot).

The fabricated biosensor was further confirmed by incubating it with a sample containing miR-204 spiked in FBS. After hybridization, the peak potential shifts to lower potential, i.e., cathodic potential of −0.108 V (E_{PC}) and anodic potential of 0.014 V(E_{PA}). Also, the corresponding peak currents of 38.22 µA and 20.8 µA, respectively (Green coloured short dash), were observed. The calculated ΔE_P value is 0.13 V which shows that the system follows Nernst equation. Also, low redox potential decreases the probability of undesirable redox reactions from other redox species (like uric and ascorbic acid) present in the sample and hence decreased interference is expected. The variation in the potential and current response after addition of the sample is indicative of the modification of the surface with gold nanoparticles and probe ssDNA.

Further, biosensor response characteristics were analyzed by cyclic voltammetric studies varying the scan rate from 10 to 150 mVs^{-1}. As observed from Fig. 4a, with increasing scan rate, the peak current increases to keep the charge constant as given by Eq. (1),

$$\text{Charge(coulomb)} = \text{current(ampere)} \times \text{time(second)}. \quad (1)$$

Also, at low scan rates, the ratio of $I_{PC}/I_{PA} < 1$ is indicative of the quasi reversible nature of the reaction, though the ratio approaches one at 100 mV/s. The plot of anodic

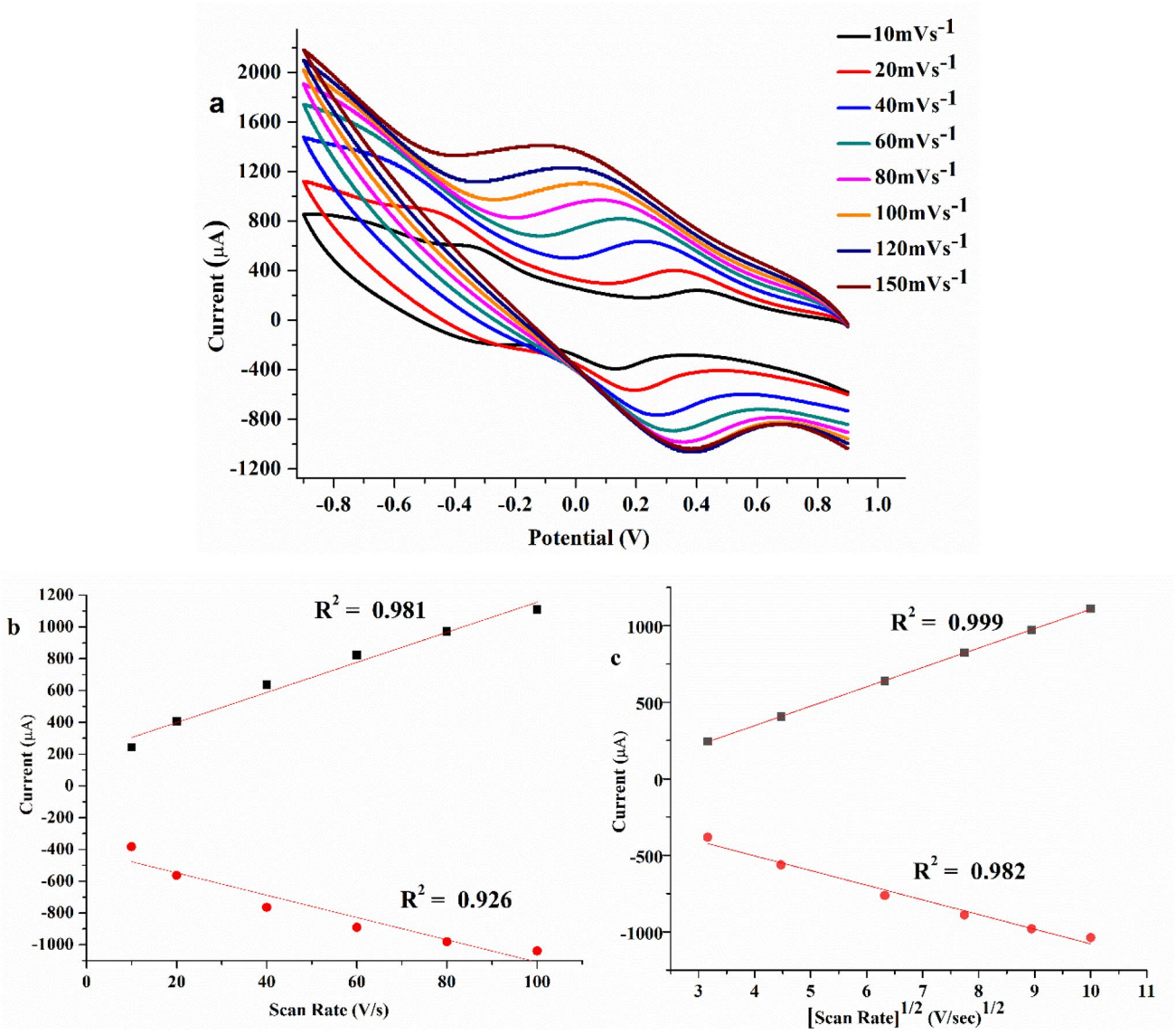

Fig. 4 **a** Cyclic voltammogram of fabricated biosensor recorded by varying scan rates for 0.1 µg of miR-204 spiked in FBS. **b** Variation of peak current as a function of scan rate and **c** variation of peak current as a function of square root of scan rate

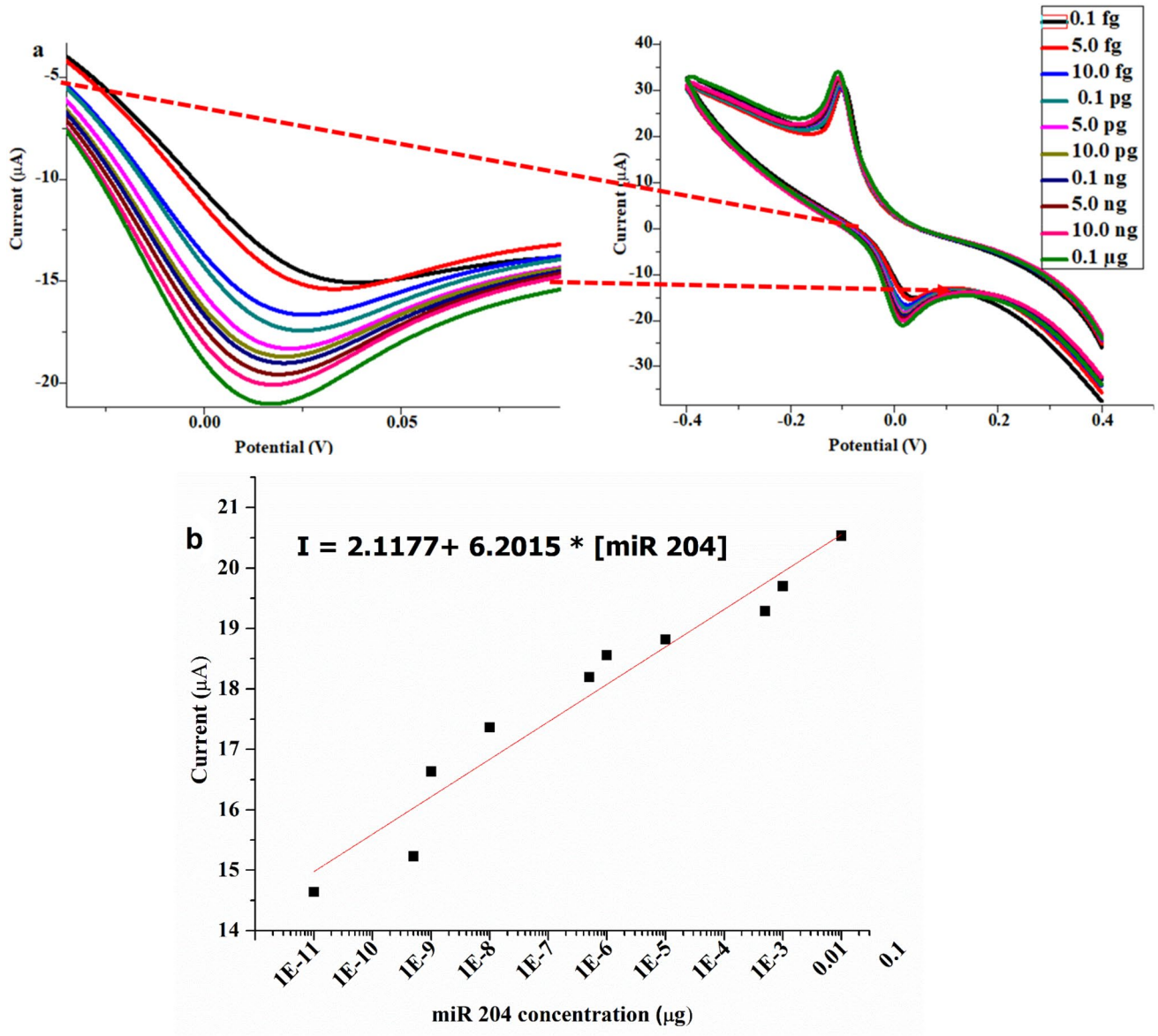

Fig. 5 **a** Cyclic voltammetry response of fabricated biosensor after hybridization with different concentrations ranging from (0.1 fg to 0.1 µg) of miR-204 spiked with FBS. **b** Calibration plot showing the peak current as a function of miR-204 concentration

and cathodic peak current as a function of scan rate (ν) and square root of scan rate ($\nu^{1/2}$) is shown in Fig. 4b and c, respectively. The linear regression analysis of the two curves shows R^2 of 0.99 for variation of peak current with $\nu^{1/2}$, while poor linear fit was observed for peak current vs scan rate ν. This suggest the reaction to be diffusion controlled.

3.3 Quantification of miR-204

Quantification of miR-204 was carried out by recording the cyclic voltammetric responses at a scan rate of 100 mV/s from − 0.4 to 0.4 V for different concentrations (0.1 fg/mL–0.1 µg/mL) spiked in fetal bovine serum (FBS) (as shown in Fig. 5a).

The peak current increases with increasing concentration of the miR-204 in sample. The cathodic peak shows poorer resolution as compared to the anodic peak. The calibration plot of anodic peak current with concentration of miR-204 is shown in Fig. 5b. Figure 5a inset shows the enlarged image of the anodic peak. The sensitivity of the fabricated biosensor having working electrode of 3 mm diameter was found to be:

Table 2 RNA-based electrochemical biosensor for detection of cancer

Cancer Type	miRNA detected	Sample	Detection methodology	Linear\Detection range	Limit of detection	Time for Hybridization	Type of Electrode Biosensor	Ref
Breast cancer	miR-21	Breast cancer cell line	DPV	–	6 pM	20 min	Graphite pencil electrode Voltammetric measurements of oxidation signals are recorded by the enzymatic reaction product	Kilic et al.[43]
General cancer	Let-7b	Hela cell lines and A549 cell lines	DPV	10 fM–0.1 nM	3.55 fM	4 h	Pd–pt supported functionalized gold SPE, triple amplification signal of redox cycling of enzyme phosphates	Chen et al. [44]
Prostate cancer	miR-141	T24 cell line	EIS and SWV	0.1 fM–0.2 pM	2.3×10^{-13} M	2 h	Methylene blue-labeled DNA probe is attached on modified SPE, dual amplification strand displacement reaction by Ca^{+2}-dependent DNAzyme	Yang, et al. [45]
General cancer	miR-21	Esophageal tumoral tissue and adjacent normal tissues collected	Chronoamperometry	10 fM–10 nM	10 fM	5 h	TSP modified gold electrode, cyclic voltammetric and amperometric detection of redox reaction by avidin-HRP or high-activity poly-HRP80	Wen et al. [46]
General cancer	miR-122b	Chemically synthesized lyophilized powder, Shanghai, China	Chronoamperometric	10 aM–1 nM	10 aM	2 h	SAM-modified surface of gold electrodes with microRNA helper, electroreduction current of miR-122b is measured by chronoamperometry	Wen et al. [47]
avian leukemia	miR-21	DF-1 chicken fibroblast cells	DPV	0.5–100 fM	0.17 fM	2 h	AuNPs-modified gold SPE, enzymatic amplification of T7 exonucleases for ultrasensitive detection of miRNAs	Ge et al. [48]
Liver cancer	miR-122	Chemically synthesized lyophilized powder	DPV	0.005–1 mM	0.1 pM	1 h	Graphite SPE, electrochemical genosensor detection of label-free guanine oxidation during hybridization of DNA–RNA	Lusi, E. A., et al [49]

Table 2 (continued)

Cancer Type	miRNA detected	Sample	Detection methodology	LinearDetection range	Limit of detection	Time for Hybridization	Type of Electrode Biosensor	Ref
General cancer	miR-155	Chemically synthesized from TaKaRa, Dalian, China	CV	5.6 pM –0.56 µM	1.87 pM	16 h	Glassy carbon electrode	Wu et al. [50]
General cancer	Let-7b	Chemically synthesized from TaKaRa, Dalian, China	Amperometry	100 pM–100 nM	3.4 aM	2 h	Modified gold SPE allosteric molecular beacons, interactions of protein–aptamer that generates electrochemical signal for displacement of complicated DNA hairpin structure	Cai et al. [51]
Breast cancer	miR-21	Chemically synthesized from Sangon, Shanghai, China	SWV	10 fM–1 nM	2.9 fM	1.5 h	Glassy carbon electrode; the SWV signals were generated by the reduction reaction of methylene blue (MB)	Ma et al. [52]

$$\text{Sensitivity} = \frac{\text{Slope of calibration plot}}{\text{Area of working electrode}} = \frac{0.62\,\mu\text{A}/\mu\text{g/ml}}{0.07\,\text{cm}^2} = 8.86\,\mu\text{g}/\mu\text{L}/\text{cm}^2. \quad (2)$$

The linear range of the biosensor was observed to be 15.5 aM–15.5 nM with lower detection limit less than 15 aM (0.1 fg/mL). Till date, to the best of our knowledge, no biosensor literature is available for miR-204; hence, we have compared the performance of the fabricated biosensor with other miRNA-based biosensor reported in literature. As shown in Table 2, the detection limit of the developed miR-204 biosensor is comparable to the best known biosensor for miRNA (miR-122b), while the linear range of the fabricated biosensor for miR-204 is much wider than that of any of the listed miRNA biosensors. The wide linear range makes it a suitable diagnostic tool for stage I to stage IV cancer.

4 Conclusion

The present study describes L-glutamic acid-synthesized gold nanoparticles which were fabricated on carbon screen-printed electrode. This modified carbon screen-printed electrode was attached with probe ssDNA. Later, to avoid non-specific interactions and matrix effects, the surface is blocked with gelatin. Next, the hybridization process is carried out by adding miR-204 for 1 h at room temperature out of 4 h of the total fabrication process. The generated current response was analysed by using cyclic voltammetry (CV). The results of this experiment showed that the proposed biosensor displays a wide linear range with lower detection limit less than 0.1 fg/mL, making it suitable for early diagnosis and prognosis of cancer. DNA-based biosensor developed using these nanoparticles can be used for detection and quantification of other interesting miRNAs in biosamples. Future research will move toward effective, easy, miniautrized, miRNA-based biosenors for clinical applications.

Acknowledegements Shilpa is thankful to Jaypee Institute of Information Technology Noida, India, for providing research assistance to complete this project. The authors are also thankful to the Advanced Instrumentation and Research Facility (AIRF), Jawaharlal Nehru University, for extending the facility for transmission electron microscopy analysis.

Funding The authors also state that there exists no financial support or funding from any sources toward this work.

Declarations

Conflict of Interest The authors state that there exists no conflict of interest toward this work.

References

1. Mathur P, Sathishkumar K, Chaturvedi M, Das P, Sudarshan KL, Santhappan S, ICMR-NCDIR-NCRP Investigator Group (2020) Cancer statistics, 2020: report from national cancer registry programme, India. JCO Glob Oncol 6:1063–1075. https://doi.org/10.1200/go.20.00122
2. Bray F, Ferlay J, Soerjomataram I, Siegel RL, Torre LA, Jemal A (2018) Global cancer statistics 2018: GLOBOCAN estimates of incidence and mortality worldwide for 36 cancers in 185 countries. Cancer J Clinicians 68(6):394–424. https://doi.org/10.3322/caac.21492
3. Ludwig JA, Weinstein JN (2005) Biomarkers in cancer staging, prognosis and treatment selection. Nat Rev Cancer 5(11):845–856. https://doi.org/10.1038/nrc1739
4. Ortiz-Quintero B (2016) Cell-free microRNAs in blood and other body fluids, as cancer biomarkers. Cell Prolifer 49(3):281–303. https://doi.org/10.1111/cpr.12262
5. Cui M, Wang H, Yao X, Zhang D, Xie Y, Cui R, Zhang X (2019) Circulating microRNAs in cancer: potential and challenge. Front Genet 10:626. https://doi.org/10.3389/fgene.2019.00626
6. Weber JA, Baxter DH, Zhang S, Huang DY, How Huang K, Jen Lee M, Wang K (2010) The microRNA spectrum in 12 body fluids. Clin Chem 56(11):1733–1741. https://doi.org/10.1373/clinchem.2010.147405
7. Rezayi M, Farjami Z, Hosseini ZS, Ebrahimi N, Abouzari-Lotf E (2018) MicroRNA-based biosensors for early detection of cancers. Curr Pharm Des 24(39):4675–4680. https://doi.org/10.2174/1381612825666190111144525
8. Xie X, Liu J, Ding M, Yang X, Peng Y, Zhao Y, Miao Y (2021) Recent development of the electrochemical sensors for miRNA detection. Int J Electrochem Sci 16(4):1–17. https://doi.org/10.20964/2021.04.35
9. Khalid M, Idichi T, Seki N, Wada M, Yamada Y, Fukuhisa H, Natsugoe S (2019) Gene regulation by antitumor miR-204–5p in pancreatic ductal adenocarcinoma: the clinical significance of direct RACGAP1 regulation. Cancers 11(3):327. https://doi.org/10.3390/cancers11030327
10. Schmeier S, Schaefer U, Essack M, Bajic VB (2011) Network analysis of microRNAs and their regulation in human ovarian cancer. BMC Syst Biol 5:183. https://doi.org/10.1186/1752-0509-5-183
11. Bao W, Wang HH, Tian FJ, He XY, Qiu MT, Wang JY, Wan XP (2013) A TrkB–STAT3–miR-204–5p regulatory circuitry controls proliferation and invasion of endometrial carcinoma cells. Mol Cancer 12:155. https://doi.org/10.1186/1476-4598-12-155
12. Li W, Jin X, Zhang Q, Zhang G, Deng X, Ma L (2014) Decreased expression of miR-204 is associated with poor prognosis in patients with breast cancer. Int J Clin Exp Pathol 7(6):3287–3292 (**PMID: 25031750; PMCID: PMC4097245**)
13. Bussemakers MJ, Van Bokhoven A, Verhaegh GW, Smit FP, Karthaus HF, Schalken JA et al (1999) DD3: a new prostate-specific gene, highly overexpressed in prostate cancer. Cancer Res 59(23):5975–5979 (**PMID: 10606244**)
14. Sümbül AT, Göğebakan B, Ergün S, Yengil E, Batmacı CY, Tonyalı Ö, Yaldız M (2014) miR-204-5p expression in colorectal cancer: an autophagy-associated gene. Tumor Biol 35(12):12713–12719. https://doi.org/10.1007/s13277-014-2596-3
15. Chen X, Liu XS, Liu HY, Lu YY, Li Y (2016) Reduced expression of serum miR-204 predicts poor prognosis of gastric cancer. Genet Mol Res 15(2):15027702. https://doi.org/10.4238/gmr.15027702
16. Fan X, Zou X, Liu C, Cheng W, Zhang S, Geng X, Zhu W (2021) MicroRNA expression profile in serum reveals novel diagnostic biomarkers for endometrial cancer. Biosci Rep 41(6):BSR20210111. https://doi.org/10.1042/BSR20210111
17. Zheng W, Huang W, Yu X (2021) Study on serum miR-204 expression levels in patients with severe pneumonia and patients with primary bronchial lung cancer and its diagnostic value. Evidence-Based Complement Alternat Med 2021:6034413. https://doi.org/10.1155/2021/6034413
18. Nie D, Ma P, Chen Y, Zhao H, Liu L, Xin D, Sun L (2021) MiR-204 suppresses the progression of acute myeloid leukemia through HGF/c-Met pathway. Hematology 26(1):931–939. https://doi.org/10.1080/16078454.2021.1981533
19. Guo W, Zhang Y, Zhang Y, Shi Y, Xi J, Fan H, Xu S (2015) Decreased expression of miR-204 in plasma is associated with a poor prognosis in patients with non-small cell lung cancer. Int J Mol Med 36(6):1720–1726. https://doi.org/10.3892/ijmm.2015.2388
20. Gaddam RR, Jacobsen VP, Kim YR, Gabani M, Jacobs JS, Dhuri K, Vikram A (2020) Microbiota-governed microRNA-204 impairs endothelial function and blood pressure decline during inactivity in db/db mice. Sci Rep 10(1):1–14. https://doi.org/10.1038/s41598-020-66786-0
21. Cheng Y, Wang D, Wang F, Liu J, Huang B, Baker MA, Liang M (2020) Endogenous miR-204 protects the kidney against chronic injury in hypertension and diabetes. J Am Soc Nephrol 31(7):1539–1554. https://doi.org/10.1681/ASN.2019101100
22. Chiu CC, Yeh TH, Chen RS, Chen HC, Huang YZ, Weng YH, Wang HL (2019) Upregulated expression of microRNA-204–5p leads to the death of dopaminergic cells by targeting DYRK1A-mediated apoptotic signaling cascade. Front Cell Neurosci 13:399. https://doi.org/10.3389/fncel.2019.00399
23. Xu G, Thielen LA, Chen J, Grayson TB, Grimes T, Bridges SL Jr, Shalev A (2019) Serum miR-204 is an early biomarker of type 1 diabetes-associated pancreatic beta-cell loss. Am J Physiol-Endocrinol Metab 317(4):E723–E730. https://doi.org/10.1152/ajpendo.00122.2019
24. Kurahashi R, Kadomatsu T, Baba M, Hara C, Itoh H, Miyata K, Oike Y (2019) MicroRNA-204–5p: a novel candidate urinary biomarker of Xp11. 2 translocation renal cell carcinoma. Cancer Sci 110(6):1897–1908. https://doi.org/10.1111/cas.14026
25. Debernardi S, Massat NJ, Radon TP, Sangaralingam A, Banissi A, Ennis DP, Crnogorac-Jurcevic T (2015) Non-invasive urinary miRNA biomarkers for early detection of pancreatic adenocarcinoma. Am J Cancer Res 5(11):3455–3466 (**PMID: 26807325**)
26. Tapia-Castillo A, Guanzon D, Palma C, Lai A, Barros E, Allende F, Carvajal CA (2019) Downregulation of exosomal miR-192–5p and miR-204–5p in subjects with nonclassic apparent mineralocorticoid excess. J Transl Med 17(1):1–11. https://doi.org/10.1186/s12967-019-02143-8
27. Hofbauer SL, de Martino M, Lucca I, Haitel A, Susani M, Shariat SF, Klatte T (2018) A urinary microRNA (miR) signature for diagnosis of bladder cancer. Urol Oncol 36(12):1–8. https://doi.org/10.1016/j.urolonc.2018.09.006
28. Scian MJ, Maluf DG, David KG, Archer KJ, Suh JL, Wolen AR et al (2011) MicroRNA profiles in allograft tissues and paired urines associate with chronic allograft dysfunction with IF/TA. Am J Transp 11(10):2110–2122. https://doi.org/10.1111/j.1600-6143.2011.03666.x
29. Ding M, Lin B, Li T, Liu Y, Li Y, Zhou X, Li R (2015) A dual yet opposite growth-regulating function of miR-204 and its target XRN1 in prostate adenocarcinoma cells and neuroendocrine-like prostate cancer cells. Oncotarget 6(10):7686–7700. https://doi.org/10.18632/Foncotarget.3480
30. Lee H, Lee S, Bae H, Kang HS, Kim SJ (2016) Genome-wide identification of target genes for miR-204 and miR-211 identifies their proliferation stimulatory role in breast cancer cells. Sci Reports 6(1):1–12. https://doi.org/10.1038/srep25287
31. Hong BS, Ryu HS, Kim N, Kim J, Lee E, Moon H, Moon HG (2019) Tumor suppressor miRNA-204-5p regulates growth,

metastasis, and immune microenvironment remodelling in breast cancer. Can Res 79(7):1520–1534. https://doi.org/10.1158/0008-5472.CAN-18-0891
32. Hoffmann A, Huang Y, Suetsugu-Maki R, Ringelberg CS, Tomlinson CR, Rio-Tsonis D, Tsonis PA (2012) Implication of the miR-184 and miR-204 competitive RNA network in control of mouse secondary cataract. Mol Med 18(3):528–538. https://doi.org/10.2119/molmed.2011.00463
33. Yin Y, Zhang B, Wang W, Fei B, Quan C, Zhang J, Huang Z (2014) miR-204-5p inhibits proliferation and invasion and enhances chemotherapeutic sensitivity of colorectal cancer cells by downregulating RAB22A. Clin Cancer Res 20(23):6187–6199. https://doi.org/10.1158/1078-0432.CCR-14-1030
34. Conte I, Hadfield KD, Barbato S, Carrella S, Pizzo M, Bhat RS, Black GC (2015) MiR-204 is responsible for inherited retinal dystrophy associated with ocular coloboma. Proc Natl Acad Sci 112(25):E3236–E3245. https://doi.org/10.1073/pnas.1401464112
35. Qiu YH, Wei YP, Shen NJ, Wang ZC, Kan T, Yu WL et al (2013) miR-204 inhibits epithelial to mesenchymal transition by targeting slug in intrahepatic cholangiocarcinoma cells. Cell Physiol Biochem 32(5):1331–1341. https://doi.org/10.1159/000354531
36. Shen SQ, Huang LS, Xiao XL, Zhu XF, Xiong DD, Cao XM et al (2017) miR-204 regulates the biological behaviour of breast cancer MCF-7 cells by directly targeting FOXA1. Oncol Rep 38(1):368–376. https://doi.org/10.3892/or.2017.5644
37. Guo J, Zhao P, Liu Z, Li Z, Yuan Y, Zhang X, Xiao K (2019) MiR-204–3p inhibited the proliferation of bladder cancer cells via modulating lactate dehydrogenase-mediated glycolysis. Front Oncol 9:1242. https://doi.org/10.3389/fonc.2019.01242
38. Ying Z, Li Y, Wu J, Zhu X, Yang Y, Tian H, Li M (2013) Loss of miR-204 expression enhances glioma migration and stem cell-like phenotype. Can Res 73(2):990–999. https://doi.org/10.1158/0008-5472.CAN-12-2895
39. Ryan J, Tivnan A, Fay J, Bryan K, Meehan M, Creevey L, Stallings RL (2012) MicroRNA-204 increases sensitivity of neuroblastoma cells to cisplatin and is associated with a favourable clinical outcome. Br J Cancer 107(6):967–976. https://doi.org/10.1038/bjc.2012.356
40. Zhang L, Wang X, Chen P (2013) MiR-204 down regulates SIRT1 and reverts SIRT1-induced epithelial-mesenchymal transition, anoikis resistance and invasion in gastric cancer cells. BMC Cancer 13:290. https://doi.org/10.1186/1471-2407-13-290
41. Findlay VJ, Turner DP, Moussa O, Watson DK (2008) MicroRNA-mediated inhibition of prostate-derived Ets factor messenger RNA translation affects prostate-derived Ets factor regulatory networks in human breast cancer. Can Res 68(20):8499–8506. https://doi.org/10.1158/0008-5472.CAN-08-0907
42. Sharma S, Gupta N, Srivastava S (2012) Modulating electron transfer properties of gold nanoparticles for efficient biosensing. Biosens Bioelectron 37(1):30–37. https://doi.org/10.1016/j.bios.2012.04.027
43. Kilic T, Topkaya SN, Ariksoysal DO, Ozsoz M, Ballar P, Erac Y, Gozen O (2012) Electrochemical based detection of microRNA, mir21 in breast cancer cells. Biosens Bioelectron 38(1):195–201. https://doi.org/10.1016/j.bios.2012.05.031
44. Cheng FF, Zhang JJ, He TT, Shi JJ, Abdel-Halim ES, Zhu JJ (2014) Bimetallic Pd–Pt supported graphene promoted enzymatic redox cycling for ultrasensitive electrochemical quantification of microRNA from cell lysates. Analyst 139(16):3860–3865. https://doi.org/10.1039/C4AN00777H
45. Yang D, Cheng W, Chen X, Tang Y, Miao P (2018) Ultrasensitive electrochemical detection of miRNA based on DNA strand displacement polymerization and Ca 2+-dependent DNAzyme cleavage. Analyst 143(22):5352–5357. https://doi.org/10.1039/C8AN01555D
46. Wen Y, Pei H, Shen Y, Xi J, Lin M, Lu N, Fan C (2012) DNA nanostructure-based interfacial engineering for PCR-free ultrasensitive electrochemical analysis of microRNA. Sci Rep 2(1):867. https://doi.org/10.1038/srep00867
47. Wen Y, Liu G, Pei H, Li L, Xu Q, Liang W, Fan C (2013) DNA nanostructure-based ultrasensitive electrochemical microRNA biosensor. Methods 64(3):276–282. https://doi.org/10.1016/j.ymeth.2013.07.035
48. Ge Z, Lin M, Wang P, Pei H, Yan J, Shi J, Zuo X (2014) Hybridization chain reaction amplification of microRNA detection with a tetrahedral DNA nanostructure-based electrochemical biosensor. Anal Chem 86(4):2124–2130. https://doi.org/10.1021/ac4037262
49. Lusi EA, Passamano M, Guarascio P, Scarpa A, Schiavo L (2009) Innovative electrochemical approach for an early detection of microRNAs. Anal Chem 81(7):2819–2822. https://doi.org/10.1021/ac8026788
50. Wu X, Chai Y, Yuan R, Su H, Han J (2013) A novel label-free electrochemical microRNA biosensor using Pd nanoparticles as enhancer and linker. Analyst 138(4):1060–1066. https://doi.org/10.1039/C2AN36506E
51. Cai Z, Song Y, Wu Y, Zhu Z, Yang CJ, Chen X (2013) An electrochemical sensor based on label-free functional allosteric molecular beacons for detection target DNA/miRNA. Biosens Bioelectron 41:783–788. https://doi.org/10.1016/j.bios.2012.10.002
52. Ma X, Xu H, Qian K, Kandawa-Schulz M, Miao W, Wang Y (2020) Electrochemical detection of microRNAs based on AuNPs/CNNS nanocomposite with Duplex-specific nuclease assisted target recycling to improve the sensitivity. Talanta 208:120441. https://doi.org/10.1016/j.talanta.2019.120441

Authors and Affiliations

Shilpa Gundagatti[1] · Sudha Srivastava[1]

Shilpa Gundagatti
shilpaishu06@gmail.com

[1] Department of Biotechnology, Jaypee Institute of Information Technology, A-10, Sector-62, Noida, U.P., India